

A Survey about Acquisition System Design for Myoelectric Prosthesis

Ahmed Naguib, Dina Reda Eldamak

December 2022

1 Introduction

According to the World Health Organization (WHO), 30 million people are in need of prosthetic and orthotic devices [1]. Some people are born with this limb loss, while others lose limbs due to diseases such as Cancer, diabetes, and work accidents. Additionally, limb amputation is among the most severe and heavily reported injuries among veterans during war [2, 3]. Example of female with hand amputation is shown in Figure 1.



Figure 1: Female with Prosthetic limb [4]

The medical applications of integrated circuit technology have recently made significant advances, thus improving human quality of life. Moreover, the use of microelectronics integration

dominates a lot of medical applications, especially portable and wearable battery-operated devices. Bio-signals mostly arise from natural physiological processes, such as cardiac potentials (ECG -electro-cardiogram), potentials of the ocular tissue (EOG - electro-oculogram), potentials of the muscular tissues (electro-myogram -EMG), brain potential (electro-encephalogram -EEG), and respiratory signals , etc. Electro-myogram - EMG is an important factor for muscle disease diagnosis. Furthermore, it's the key factor in connecting any amputee to a prosthetic limb. This can be done through extracting the EMG signal from the body using a readout electronics that can detect the muscles electrical activity. Consequently, the extracted signal is processed and used to control the prosthetic limb. Thus, the objective of this report is to provide the reader with the basic understanding of integrated solutions for controlling prosthetic limbs either arms or legs.

The top level block diagram of a smart EMG acquisition system is shown in Fig. 2. The system includes a self-powered readout portable acquisition device for measuring the patient's EMG signal in order to send it to a controller that can be used to emulate the right action to the prosthetic limb similar to the same action in a normal person. It should be noted that miniaturized EMG acquisition system idea, which continuously monitor muscles activity, can be extended to different applications such as physical rehabilitation and prosthesis.

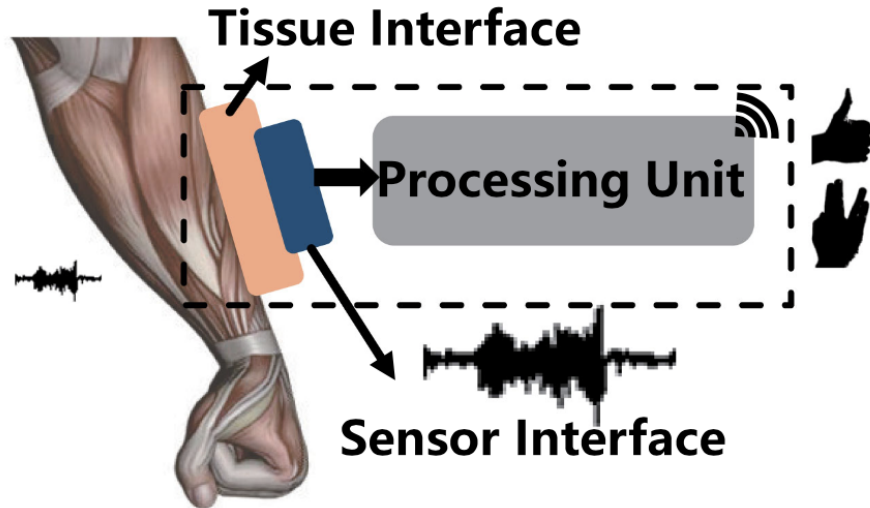


Figure 2: Block diagram of a general smart sEMG recorder [5]

2 System Architecture

An electronic system can control a prosthetic device by monitoring the EMG signals of the arm, and use those signals to control the prosthetic arm. Moreover, the devices can be battery-free by being powered solely using energy harvesting from the ambient.

Since these prosthetic devices requires precise fitting to the residual limb, pressure and temperature sensor at the skin-prosthetic interface are added to the system. Pressure sensors are needed for monitoring the prosthetic limb to avoid the development of regions of high pressure as the limb moves during walking or grasping objects. Temperature sensor are necessary as high temperature can accelerate tissue damage [6]. The signals from the sensor at the skin-prosthetic can be transmitted to the outer surface of the prosthetic socket using Near Field Communication (NFC) or to a smart phone using Bluetooth Low Energy (BLE) as shown in Figure 3.

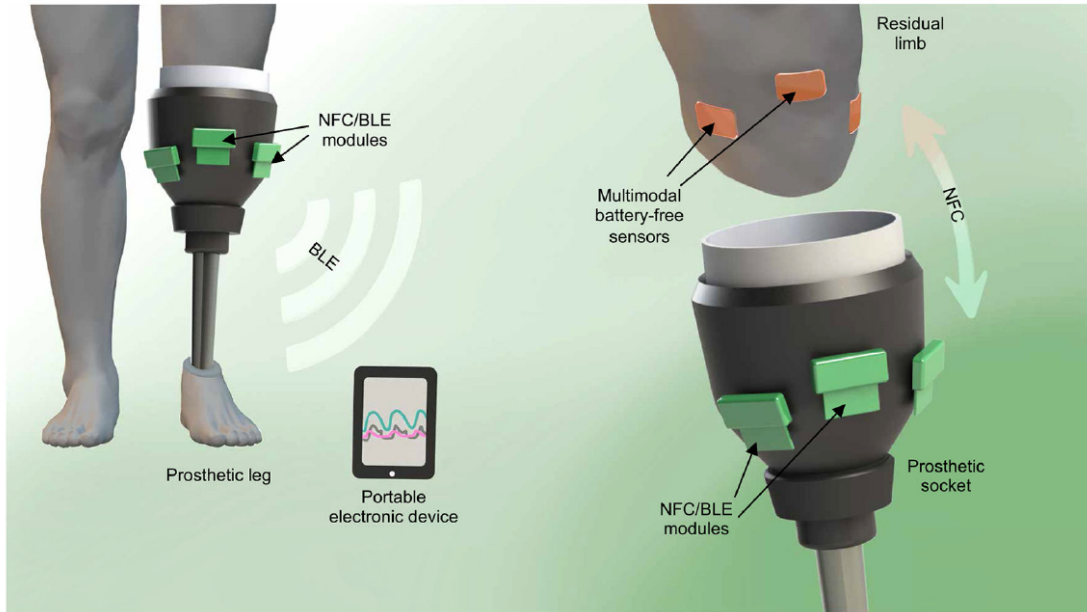


Figure 3: Illustration of sensors mounted at the skin-prosthetic interface transmitting data to the device at the outer surface of the prosthetic leg using NFC and to smart phone using BLE [6].

3 Block Diagram

Three major research directions are available when designing an EMG acquisition system. The first is to acquire the signal from the surrounding noisy environment using a sensor interface

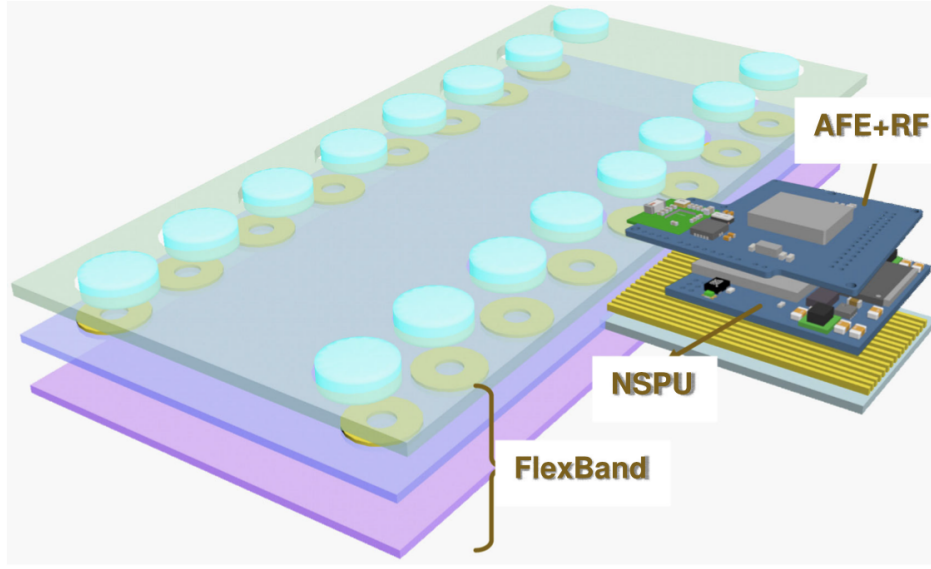


Figure 4: Block diagram of the proposed smart sEMG recorder including sensors, AFE, and RF integrated system [5]

circuit that's designed in CMOS technology. The second involves reducing the form factor and power consumption of the acquisition system. The third is the signal conversion to the digital world and the interface with the digital controller. At this point, the extracted EMG signal is in a digital form and can be processed through FPGA or any other processor to control a Prosthetic limb.

A typical block diagram of the proposed EMG acquisition system is shown in Fig. 4. The system consists of an EMG sensor, analog front end (AFE), and radio frequency (RF) transmission unit. The AFE is typically composed of an analog amplification, filtration, analog to digital converter (ADC), and controller to process the digital signal and send it to a prosthetic limb. The acquisition system design can be integrated on a single chip, then the digital data is fed to FPGA or a controller.

In addition, because the integrated solution takes a considerable time during design, fabrication, and testing phases, a discrete solution in parallel with the integrated one can be used as a proof of concept to validate the proposed methodology.

Figure 5 shows a detailed system block diagram of the proposed smart sEMG acquisition system. An analog multiplexer is inserted to choose between different EMG electrodes in the smart sEMG recorder shown in the figure. The design of each of the building blocks involves

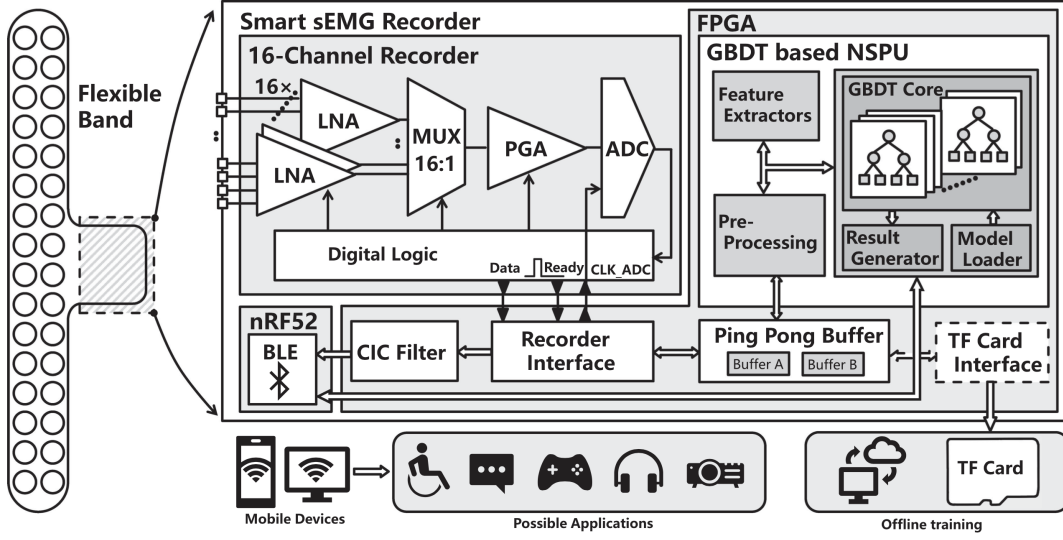


Figure 5: Detailed block diagram of the proposed smart sEMG acquisition system [5]

several design challenges requiring some research. The following section includes a list of major research directions that can be pursued.

4 Circuit Implementation

In the following subsections, the basic system building blocks are introduced. First, the EMG sensor specifications are explored. Second, the low noise amplifier LNA design is presented. Third, the filter design and bandwidth are provided. Fourth, the signal conversion from analog to digital is presented through an ADC. Last, digital signal processing through FPGA is explored.

4.1 Sensor Specifications

EMG sensor placement plays an important role in signal acquisition. According to its orientation and position, the EMG signal strength varies significantly. This effect is shown in Fig 6. As seen, by placing the sensor in the middle of muscle fiber, the maximum signal strength can be easily obtained. Otherwise, the signal degrades significantly when placing the sensor far away from the middle.

EMG sensor can be represented in different forms. It can be in either needle that is inserted into the muscle or surface electrode that picks the signal from the skin. An example of surface

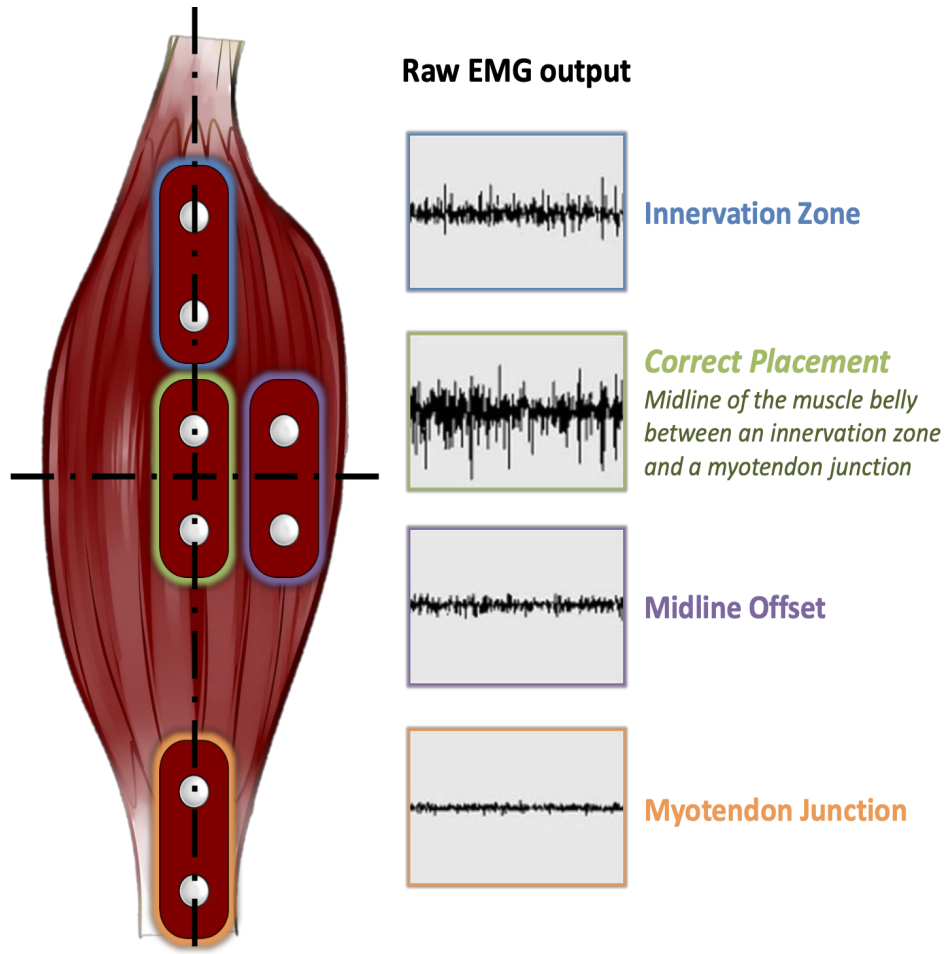


Figure 6: Effect of EMG sensor position [7]

EMG sensor specifications that have to be met through out the design are as follow shown in Fig. 7.

4.2 Low Noise Amplifier Design

It's the first and the major block in the EMG chain that comes after the sensor. The measurement sensitivity and accuracy is determined in this stage. This complicates the design and requires a large amount of adaptability to accommodate the input signal. The previous stage, which is the EMG sensor, adds large parasitic capacitance at the input of this stage, and thus reduces gain, bandwidth, noise performance and the sensitivity of the amplifier.

Sources of noise and interference like flicker noise, electrodes offset, and 60 Hz power line noise can affect the whole acquisition procedure. The bandwidth of the EMG signal is up to

	DataLITE Wireless EMG Amplifier	Wired EMG Amplifier
Product Ref	LE230FW	SX230FW
Dimensions	42 x 24 x 14 mm Two 4 mm snap connectors on 100 mm wires	38 x 20 Two 4 mm snap connectors on 100 mm wires
Mass	17 g (excluding cable and plug)	8g (excluding cable and plug)
Bandwidth	10 – 250, 470, 950, 5000Hz	20 – 460Hz
Additional Bandwidths	N/A	5Hz – 480Hz 5Hz – 1000Hz
Contact Diameter	Dependant on electrode size	
Contact Center Spacing	Variable	
Electrodes	Disposable	
CMRR @ 60 Hz (dB)	> 96 dB (typically 110 dB)	
Full Scale	+/- 6 mV Peak to Peak	+/- 3 mV Peak to Peak
Gain	+/- 60 microvolts to +/- 6 millivolts	Standard unit x1000 (100 also available)
Input Impedance	>100 Mohms	
Accuracy	+/- 1.0%	+/- 2% full scale
Noise	< 5 μ V	
Supply Voltage	N/A	+3.50 to +5.5 Vdc
Battery Life	Up to 8 hours	N/A
Battery Type	Rechargeable Li-Ion Polymer	N/A
Wireless Transmission Data Loss	Tolerant for 100 mS	N/A
Range from Interface	Wireless range up to 30m	1.25m cable (custom lengths available on request)
Compatible Interfaces	DataLITE PIONEER, ADVANCE, EXPLORE	DataLOG, DataLINK, Amplifier or 3 rd party

Figure 7: sensor specifications [8]

500 Hz with amplitude that ranges from 0.1 to 5 mV and the high-frequency noise can be easily removed using a low pass filter. However, low-frequency noise and DC offset fall within the EMG bandwidth and hence require different rejection techniques. Chopping technique is one of the best candidates to modulate the offset and flicker noise to a higher spectrum which in turn enable the acquisition system to effectively suppress the interference from ambient and 1/f noise. Different architectures with different requirements in terms of input signal levels, BW and amplitudes are proposed in literature [9, 10]. Figure 8 shows the block diagram of implemented analog front-end for acquiring of EEG, ECG, and EMG signals [9]. The shown diagram consists of a chopper instrumentation amplifier in addition to capacitive coupling, filter stage to remove the chopping spikes, a digitally controlled variable gain amplifier.

4.3 Filter Design

A Gm-C filter can be used in the design. A standard architecture is shown in Figure 9. Offset from the electrodes can be canceled using current-mode DAC [11]. Power Consumption of this

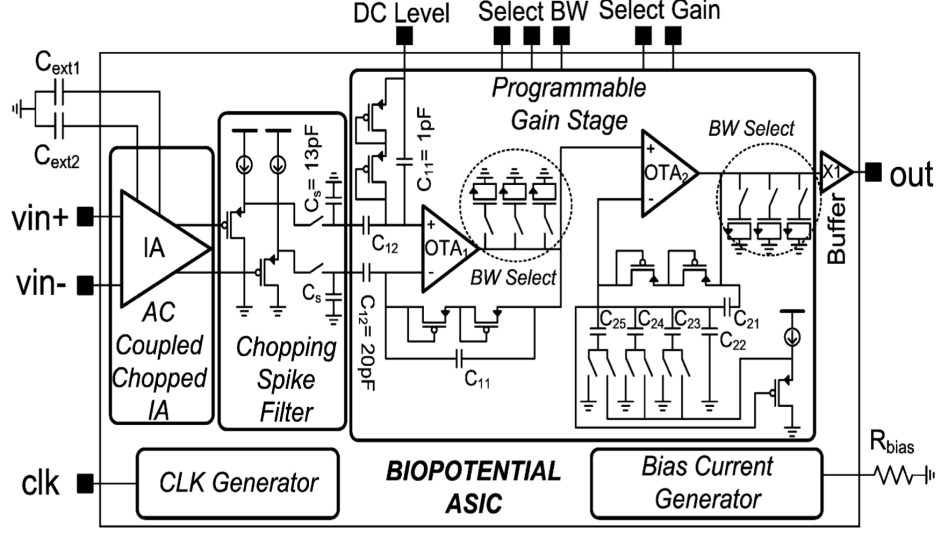


Figure 8: Architecture of the bio-potential readout front-end for the acquisition of EEG, ECG, and EMG signals [9]

topology can also be reduced by low-voltage supply operation [10].

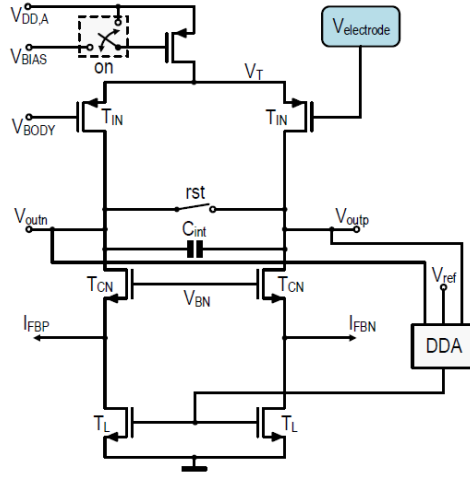


Figure 9: Transistor level implementation of Gm-C filter. DDA: Differential Difference Amplifier [11].

4.4 ADC Design

Non-uniform sampling can minimize the power consumption of ADC while digitizing activity-dependent biological signals. For example, a continuous-time (CT) charge-based ADC that ac-

quires samples when the input crosses a specific threshold is shown in Figure 10. The ADC works by storing the analog equivalent of the last digitized input as a voltage across the capacitor C_b . Once the input signal crosses this voltage, a pulse with length T_P is generated to charge or discharge the capacitor C_b by V_{LSB} using one of the current sources connected to the supply and ground [12]. Non-uniform sampling adapts to the instantaneous bandwidth of the signal, consequently the dynamic power consumption scales with the activity of the input signal. The FOM of the CT charge-based ADC can be improved by reducing the power supply further [10].

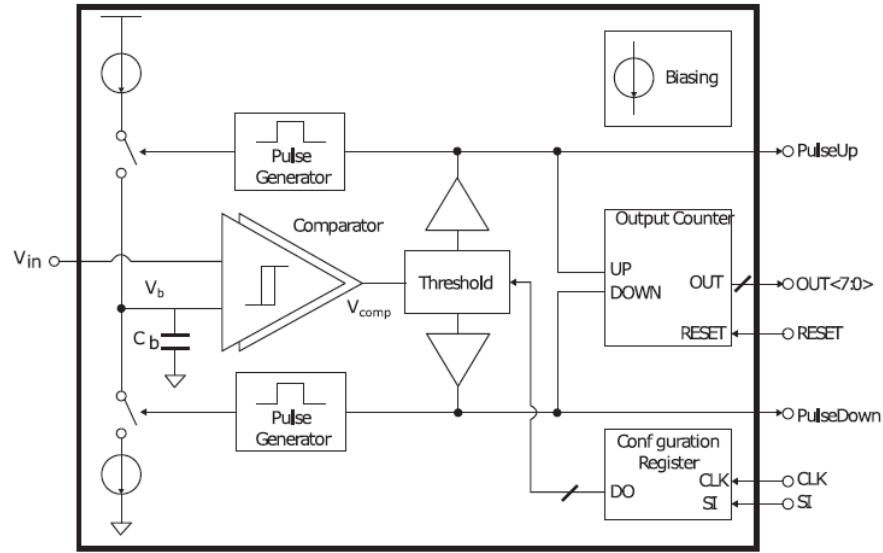


Figure 10: Top level architecture of Continuous-time (CT) charge based ADC with non-uniform sampling rate [12].

4.5 FPGA Processing

Machine learning algorithms such as Support Vector Machine (SVM) have allowed for on-chip feature extraction and classification of biomedical signals [13]. Machine learning can also be deployed in the domain of prosthetic devices for precise control. Figure 11 depicts the controller of prosthetic device which can be implemented using Field Programmable Gate Array (FPGA). Figure 12 depicts the experimental setup for analyzing the data from high density EMG acquisition system using Xilinx Zedboard [14].

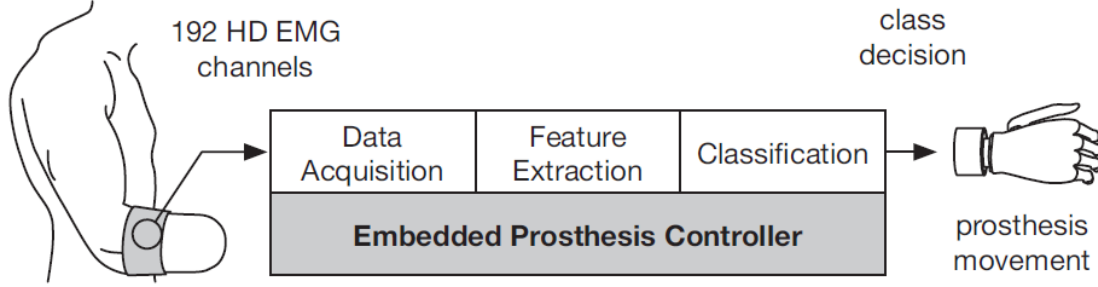


Figure 11: Top level architecture of controller of prosthetic hand including feature extraction and classification [14].

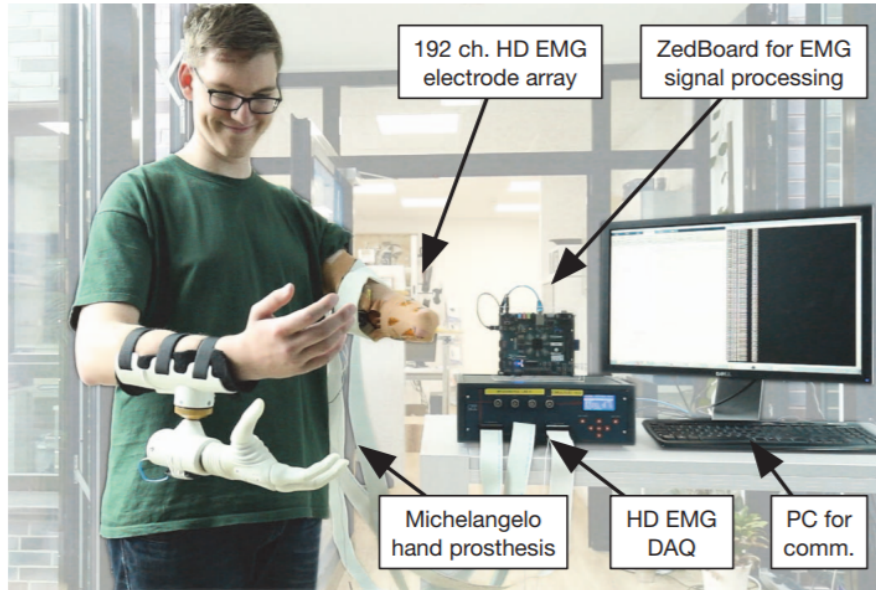


Figure 12: Experimental Setup of EMG acquisition and processing using Xilinx ZedBoard [14].

4.6 Energy Harvesting

The electrical power harvested from the environment (specially, thermal energy) can power the ultra-low-power EMG Sensor. We have previously developed energy harvesting systems from various sources and high-efficiency DC-DC converters [15, 16]. For example, the system architecture of power management IC for solar energy harvesting applications, designed by the author, and chip micrograph are shown in Figure 13.

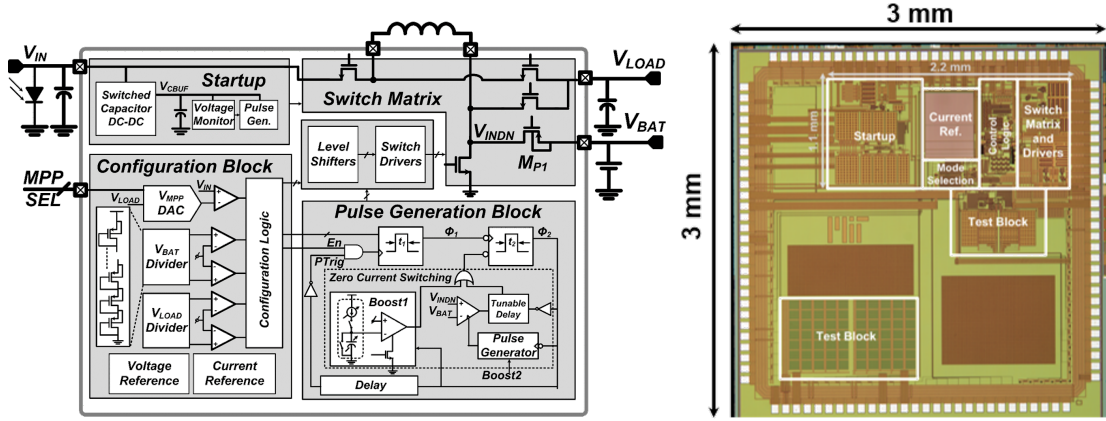


Figure 13: System architecture of power management IC for solar energy harvesting applications, designed by one of the team members, and chip micrograph [15]

5 Conclusion

This paper provided a survey about EMG acquisition systems for prosthetics and orthotic devices.

References

- [1] Shirley Ryan AbilityLab. Facts about limb loss. [Online]. Available: <https://www.sralab.org/research/labs/bionic-medicine/news/facts-about-limb-loss>
- [2] UK Ministry of Defence. Uk service personnel amputations: financial year 2019/2020. [Online]. Available: <https://www.gov.uk/government/statistics/uk-service-personnel-amputations-financial-year-20192020/afghanistan-and-iraq-amputation-statistics-1-april-2015-to-31-march-2020>
- [3] L. G. Stansbury, S. J. Lalliss, J. G. Branstetter, M. R. Bagg, and J. B. Holcomb, "Amputations in U.S. military personnel in the current conflicts in Afghanistan and Iraq," *Journal of Orthopaedic Trauma*, vol. 22, no. 1, pp. 43–46, 2008. [Online]. Available: <https://journals.lww.com/00005131-200801000-00009>
- [4] iStock . Image of a female with a prosthetic limb. [Online]. Available: <https://www.istockphoto.com/>
- [5] W. Song, Q. Han, Z. Lin, N. Yan, D. Luo, Y. Liao, M. Zhang, Z. Wang, X. Xie, A. Wang

- et al.*, “Design of a flexible wearable smart sEMG recorder integrated gradient boosting decision tree based hand gesture recognition,” *IEEE transactions on biomedical circuits and systems*, vol. 13, no. 6, pp. 1563–1574, 2019.
- [6] J. W. Kwak, M. Han, Z. Xie, H. U. Chung, J. Y. Lee, R. Avila, J. Yohay, X. Chen, C. Liang, M. Patel, I. Jung, J. Kim, M. Namkoong, K. Kwon, X. Guo, C. Ogle, D. Grande, D. Ryu, D. H. Kim, S. Madhupathy, C. Liu, D. S. Yang, Y. Park, R. Caldwell, A. Banks, S. Xu, Y. Huang, S. Fatone, and J. A. Rogers, “Wireless sensors for continuous, multimodal measurements at the skin interface with lower limb prostheses,” *Science Translational Medicine*, vol. 12, no. 574, p. eabc4327, 2020. [Online]. Available: <https://www.science.org/doi/abs/10.1126/scitranslmed.abc4327>
- [7] MyoWare, “3-lead muscle / electromyography sensor for microcontroller applications.” [Online]. Available: <https://www.mouser.com/datasheet/2/813/MyowareUserManualAT-04-001-1223951.pdf>
- [8] B. Ltd, “Surface emg amplifier.” [Online]. Available: <https://www.biometricsltd.com/surface-emg-sensor.htm#popupSpecAmplifier>
- [9] R. F. Yazicioglu, “A $60\mu\text{W}$ $60\text{ nV}/\sqrt{\text{Hz}}$ readout front-end for portable biopotential acquisition systems,” in *IEEE International Solid-State Circuits Conference Digest of Technical Papers, Feb. 2006*, 2006.
- [10] S. Orguc, H. S. Khurana, H.-S. Lee, and A. P. Chandrakasan, “0.3 v ultra-low power sensor interface for emg,” in *ESSCIRC 2017-43rd IEEE European Solid State Circuits Conference*. IEEE, 2017, pp. 219–222.
- [11] D. Wendler, D. D. Dorigo, M. Amayreh, A. Bleitner, M. Marx, and Y. Manoli, “A 0.00378mm^2 scalable neural recording front-end for fully immersible neural probes based on a two-step incremental delta-sigma converter with extended counting and hardware reuse,” in *2021 IEEE International Solid- State Circuits Conference (ISSCC)*, vol. 64, 2021, pp. 398–400.
- [12] M. Maslik, Y. Liu, T. S. Lande, and T. G. Constandinou, “Continuous-time acquisition of biosignals using a charge-based ADC topology,” *IEEE Transactions on Biomedical Circuits and Systems*, vol. 12, no. 3, pp. 471–482, 2018.

- [13] J. Yoo, L. Yan, D. El-Damak, M. A. B. Altaf, A. H. Shoeb, and A. P. Chandrakasan, "An 8-channel scalable EEG acquisition soc with patient-specific seizure classification and recording processor," *IEEE Journal of Solid-State Circuits*, vol. 48, no. 1, pp. 214–228, 2013.
- [14] A. Boschmann, G. Thombansen, L. Witschen, A. Wiens, and M. Platzner, "A zynq-based dynamically reconfigurable high density myoelectric prosthesis controller," in *Design, Automation & Test in Europe Conference & Exhibition (DATE), 2017*. IEEE, 2017, pp. 1002–1007. [Online]. Available: <http://ieeexplore.ieee.org/document/7927137/>
- [15] D. El-Damak and A. P. Chandrakasan, "A 10 nW-1 μ W power management ic with integrated battery management and self-startup for energy harvesting applications," *IEEE Journal of Solid-State Circuits*, vol. 51, no. 4, pp. 943–954, 2016.
- [16] P. Garcha, D. El-Damak, N. Desai, J. Troncoso, E. Mazotti, J. Mullenix, S. Tang, D. Trombly, D. Buss, J. Lang, and A. Chandrakasan, "A 25 mV-startup cold start system with on-chip magnetics for thermal energy harvesting," in *ESSCIRC 2017 - 43rd IEEE European Solid State Circuits Conference*, 2017, pp. 127–130.